BJ Cell

Biochem. J. (2014) **458**, 513–523 (Printed in Great Britain) doi:10.1042/BJ20131451





online data

# A dual-targeted aminoacyl-tRNA synthetase in *Plasmodium falciparum* charges cytosolic and apicoplast tRNA$^{Cys}$

James S. PHAM*, Reiko SAKAGUCHI†, Lee M. YEOH*‡, Nilushi S. DE SILVA*[1], Geoffrey I. McFADDEN‡, Ya-Ming HOU† and Stuart A. RALPH*[2]

*Department of Biochemistry and Molecular Biology, Bio21 Molecular Science and Biotechnology Institute, The University of Melbourne, Melbourne, VIC 3010, Australia
†Department of Biochemistry and Molecular Biology, Thomas Jefferson University, Philadelphia, PA 19107, U.S.A.
‡School of Botany, The University of Melbourne, Melbourne, VIC 3010, Australia

*Plasmodium* parasites possess two endosymbiotic organelles: a mitochondrion and a relict plastid called the apicoplast. To accommodate the translational requirements of these organelles in addition to its cytosolic translation apparatus, the parasite must maintain a supply of charged tRNA molecules in each of these compartments. In the present study we investigate how the parasite manages these translational requirements for charged tRNA$^{Cys}$ with only a single gene for CysRS (cysteinyl-tRNA synthetase). We demonstrate that the single *Pf*CysRS (*Plasmodium falciparum* CysRS) transcript is alternatively spliced, and, using a combination of endogenous and heterologous tagging experiments in both *P. falciparum* and *Toxoplasma gondii*, we show that CysRS isoforms traffic to the cytosol and apicoplast. *Pf*CysRS can recognize and charge the eukaryotic tRNA$^{Cys}$ encoded by the *Plasmodium* nucleus as well as the bacterial-type tRNA encoded by the apicoplast genome, albeit with a preference for the eukaryotic type cytosolic tRNA. The results of the present study indicate that apicomplexan parasites have lost their original plastidic cysteinyl-tRNA synthetase, and have replaced it with a dual-targeted eukaryotic type CysRS that recognizes plastid and nuclear tRNA$^{Cys}$. Inhibitors of the *Plasmodium* dual-targeted CysRS would potentially offer a therapy capable of the desirable immediate effects on parasite growth as well as the irreversibility of inhibitors that disrupt apicoplast inheritance.

Key words: alternative splicing, aminoacylation, aminoacyl-tRNA synthetase, apicoplast, Apicomplexa, dual-targeted, *Plasmodium*, *Toxoplasma gondii*, trafficking, tRNA.

## INTRODUCTION

aaRSs (aminoacyl-tRNA synthetases) are essential for protein translation and ensure the fidelity of translation from nucleic acid to amino acid sequence. These enzymes catalyse the correct attachment of an amino acid to its cognate tRNA, forming aminoacyl-tRNAs that can be used as substrates for codon/anticodon recognition and amino acid polymerization by the ribosome [1]. Recognition of the correct amino acid and cognate tRNA are crucial to the function of aaRSs. This specificity is achieved via two means: fidelity in substrate recognition and selective editing of incorrectly synthesized aminoacyl-tRNAs [2]. To preferentially select the correct amino acid, recognition can be achieved by shape or by induced fit [3]. In some cases discrimination is aided through the use of metal ions, such as a zinc ion for cysteine residue recognition [4]. Additionally, the binding of the proper tRNA can also increase the correct selection of the amino acid, as seen for glutaminyl-tRNA synthetase in *Escherichia coli* [5].

In eukaryotes, translation occurs in mitochondria, plastids and the cytosol. Translation in each of these compartments requires aaRSs. With few exceptions, organellar aaRSs are encoded in the nuclear genome, translated in the cytosol and post-translationally targeted to their destination. Despite the considerable evolutionary distance between the bacteria that gave rise to mitochondria ($\alpha$-proteobacteria) and plastids (cyanobacteria), a specific tRNA found in these endosymbiotic organelles is sometimes sufficiently similar to the corresponding tRNA in the other organelle that a dual-targeted aaRS can recognize and charge the tRNA in both organelles [6]. Indeed, many organellar aaRSs in *Arabidopsis* are coded by a single nuclear gene whose gene products are shared between mitochondria and plastids [7,8]. Differences between nuclear (eukaryotic)- and organelle (bacterial)-type tRNA molecules are more profound, and fewer cases exist for aaRSs being shared between endosymbiotic organelles and the cytosol. Instances of sharing include an alternatively spliced IleRS (isoleucyl-tRNA synthetase) that is shared between the cytosol and mitochondrion in *Trypanosoma* [9], a GlnRS (glutaminyl-tRNA synthetase) shared between the *Saccharomyces cerevisiae* cytosol and mitochondria [10], an alternatively-spliced LysRS (lysyl-tRNA synthetase) shared between human cytosol and mitochondria [11], and several *Arabidopsis thaliana* aaRSs shared between the cytosol and organelles [7,12].

The causative agent of severe malaria, *Plasmodium falciparum*, has three translationally active compartments. In addition to translation in the cytosol and mitochondrion, the parasite possesses a plastid obtained through secondary endosymbiosis [13], referred to as the apicoplast. Like plants, *Plasmodium* encodes too few aaRSs to serve each compartment with its own set of 20 unique enzymes [14,15]. However, unlike plant chloroplasts, the apicoplast resides in the endomembrane system [16], so mechanisms for dual targeting identified in primary

Abbreviations: aaRS, aminoacyl-tRNA synthetase; ACP, acyl carrier protein; CRT, chloroquine-resistance transporter; CysRS, cysteinyl-tRNA synthetase; HA, haemagluttinin; *Pf*CysRS, *Plasmodium falciparum* CysRS; *Tg*CysRS, *Toxoplasma gondii* CysRS.

[1] Present address: Department of Microbiology and Immunology, Columbia University Medical Center, New York, NY 10032, U.S.A.
[2] To whom correspondence should be addressed (email saralph@unimelb.edu.au).

chloroplasts cannot be directly shared or co-inherited. Whereas the transit peptides of primary chloroplasts and mitochondria are rather similar, apicoplast targeting is mediated by a very different sequence: a bipartite leader consisting of a signal peptide followed by a transit peptide [16,17]. Hence, apicoplast trafficking sequences are very unlikely to function as mitochondrial import elements, or to allow easy partitioning between apicoplast and cytosol.

A number of *Plasmodium* aaRSs that are dual-targeted to the apicoplast and the cytosol have now been identified [18,19], and a handful of similar enzymes have been identified in the related parasite *Toxoplasma gondii* [20]. However, the means of dual targeting is unclear in each case. *P. falciparum* possesses only one CysRS (cysteinyl-tRNA synthetase) (*Pf*CysRS) and we show in the present study, using a series of stable transgenic parasites, that this enzyme is dual-targeted to the cytosol and apicoplast through alternative splicing to produce isoforms with and without bipartite apicoplast-targeting presequences. Although alternative splicing has been observed before in *Plasmodium*, to our knowledge this is the first demonstration of differential localization through alternative splicing in *Plasmodium* species, and the first report of alternative splicing mediating dual targeting to a complex plastid of secondary endosymbiotic origin. No mitochondrial fraction is observed for this protein, which confirms that aminoacylation of tRNAs to be used in mitochondria must occur outside the organelle in *Plasmodium,* by a mechanism not yet understood.

As noted above, aminoacylation of organellar and nuclear tRNAs presents a potential challenge, as the tRNAs resident in these compartments are separated by more than a billion years of divergence. We show through phylogenetic analysis that the *Pf*CysRS is of eukaryotic rather than organellar origin, and that it has displaced the bacterial version in the apicoplast organelle. Despite this ancient divergence, we show that the eukaryotic-type *Pf*CysRS is able to rescue an *E. coli cysRS* mutant, demonstrating that the enzyme can recognize and can charge bacterial $tRNA^{Cys}$. In addition, using a specific *in vitro* aminoacylation assay, we confirm that recombinant *Pf*CysRS charges its cognate cytosolic $tRNA^{Cys}$, while also displaying an ability to cross charge both apicoplast and *E. coli* $tRNA^{Cys}$, although the activity with the apicoplast tRNA was lower relative to the cytosolic $tRNA^{Cys}$.

aaRSs in both the cytosol and the apicoplast of *Plasmodium falciparum* have been pursued as targets for inhibitors that could potentially be exploited to design novel antimalarial drugs [18,21,22]. Demonstration that the *Pf*CysRS is dual-targeted and can cross charge both the cytosolic and the apicoplast $tRNA^{Cys}$ suggests that inhibition of this enzyme might achieve more profound growth perturbations through disruption of both translation machineries in the parasite.

## MATERIALS AND METHODS

### Characterization of the CysRS locus

The sequence of the annotated *Pf*CysRS (PF3D7_1015200.1) was obtained from PlasmoDB [23] (http://www.plasmodb.org). Putative orthologues were retrieved using BLAST searches [24] of the GenBank® non-redundant [25] and orthoMCL [26] databases. Bioinformatic analysis of the N-terminal targeting sequence was conducted using SignalP v4.0 [27], apicoplast transit peptide predictors PATS version 1.2.1 [28] and PlasmoAP [29], as well as manual inspection of residues. Parsimony and neighbour-joining distance trees were constructed using the PHYLIP tools [30] implemented at the mobile webserver [31]. Maximum-likelihood trees were constructed using the PhyML algorithm [32].

*Pf*CysRS transcripts were characterized using RNA isolated from *P. falciparum* cultures as described previously [33] and converted into cDNA according to the Omniscript Reverse Transcription kit protocol (Qiagen). Oligonucleotide pairs corresponding to multiple possible splice junctions were designed for the locus, and final amplification of the apicoplast and cytosolic *Pf*CysRS isoforms was conducted using the primer pairs 5′-TGGAATTTTCTTGTATTTATCAAATTC-3′/3′-AAAGCTA-ACATATGTTCTTGCATGTCC-5′ and 5′-ATGAAAACATAC-TGTTACTAATATTAC-3′/3′-AAAGCTAACATATGTTCTTGC-ATGTCC-5′ respectively. PCR-amplification of genomic DNA by the oligonucleotide pairs was performed for comparison. Sequencing was conducted at the Applied Diagnostic Unit, The University of Melbourne, Melbourne, Australia.

### Construction of parasite transfection vectors

To determine the subcellular localization of the two *Pf*CysRS mRNA isoforms, two C-terminal GFP fusions were created using a pGlux.1 plasmid as described previously [34]. *P. falciparum* cDNA was amplified to create truncated N-terminal regions of the two mRNA gene isoforms and introduced into XhoI/KpnI restriction sites of pGlux.1 using the primers 5′-CCGctcgag-CGGATGAATCTTTTCCTTTTTATATGTATAGC-3′/5′-CGGg-gtaccAAAGCTAACATATGTTCTTGCATGTCC-3′ for the longer predicted apicoplast targeting transcript, and 5′-CCGctcg-agCGGATGGATAATGCTAATAAATTACC-3′/5′-CGGgtaccA-AAGCTAACATATGTTCTTGCATGTCC-3′ for the predicted cytosolic targeting transcript (letters in lower case indicate the restriction sites).

To generate a construct for epitope tagging of the endogenous *Pf*CysRS locus, we used a modified version of the pHA3 plasmid as described previously [35]. A targeting sequence to allow recombination into the *Pf*CysRS locus was created by cloning the terminal 3′-end 760 bp of the coding region in front of a triple HA (haemagluttinin) (3×HA) tag into the BglII and PstI sites, using the primers 5′-GAagatctAAGTAGGTATAATACAAAGTGGGC-3′/5′-TGCActgcagCCACTATTTTTATCAACCCATTAAGCA-3′ (letters in lower case indicate the restriction sites).

### *Plasmodium* culture and transfection

*Plasmodium falciparum* parasites (3D7 strain) were maintained in $O^+$ human erythrocytes (Australian Red Cross Blood Services, Melbourne, Australia) using a modification [18] of the method established by Trager and Jensen [36]. Transfections of ring-stage *P. falciparum* parasites with 100 $\mu$g of purified plasmid DNA were performed as described previously [37] and were grown in the presence of 5 nM WR99210 to select transfectants. For 3′ integration vectors, plasmids were cycled on and off WR99210 to obtain stable recombinant parasites.

### *Toxoplasma* culture and transfection

*T. gondii* ΔKU80 tachyzoites were kindly supplied by Dr Giel van Dooren (Research School of Biology, Australian National University, Canberra, Australia), and were cultured on human foreskin fibroblasts according to the method of Striepen and Soldati [38]. A 1.4 kb fragment of the *Tg*CysRS (*T. gondii* CysRS) 3′ end was amplified by PCR from genomic DNA using the primers TgCysRS-LIC SP (5′-TACTTCCAATCCAATTTAGC-AACGAGCAAAGGAACTGAAGG-3′) and TgCysRS-LIC ASP (5′-TCCTCCACTTCCAATTTTAGCAGTGTGTCCTTGAGA-CGCGA-3′) and inserted into the pLIC-HA3/DHFR plasmid

(a gift from Dr Michael White, University of South Florida, Tampa, FL, U.S.A.) as described previously [39]. Parasites were transfected as described in [38], with selection in 1 $\mu$M pyrimethamine, using resistance conferred by a *T. gondii*-specific mutation of dihydrofolate reductase [40]. Parasites were cloned by limiting dilution as described in [38], before being analysed by Western blotting and immunofluorescence assay.

#### Epifluorescence microscopy

Live-cell imaging of the *Pf*CysRS-$A_{1-153}$GFP and *Pf*CysRS-$B_{1-70}$GFP transfectants was performed using a Zeiss Axioplan2 epifluorescence microscope as described previously [41]. To determine the subcellular trafficking of *Pf*CysRS-tagged transfectants, immunofluorescence assays were performed as described in [42]. After fixation and permeabilization, samples were incubated in 3 % BSA containing rat anti-HA (1:200 dilution, Roche), rabbit anti-ACP (acyl carrier protein) (1:500 dilution [16]), mouse anti-GFP (1:200 dilution, Roche) and rabbit anti-CysRS (1:500 dilution) primary antibodies. Alexa Fluor® 488- and Alexa Fluor® 594-conjugated secondary antibodies (1:1000 dilution, Molecular Probes) diluted with 3 % BSA were used. Samples were incubated in combinations of the antibodies before mounting. Cells were visualized by epifluorescence microscopy, by 3D reconstruction using a DeltaVision Elite imaging system, and by confocal microscopy using a Leica SP5 laser-scanning confocal microscope. Localization experiments using a rabbit anti-CysRS antibody were performed with an apicoplast protein, *Pf*RRF1 (PF3D7_0208600), with a GFP tag used as a marker for the apicoplast. To specifically visualize labelling inside the apicoplast, parasite membranes were differentially solubilized and cytosolic contents extracted as described previously [18].

#### Anti-CysRS antibody

A peptide corresponding to the 14 C-terminal amino acids of the *Pf*CysRS protein (AGDQKKGNQNEKRE) conjugated to KLH (keyhole limpet haemocyanin) at the N-terminus of the peptide, was used to immunize rabbits for production of affinity-purified antibodies using a commercial antibody service (GenScript Corporation).

#### Western blot analysis

Western blots on parasite-derived protein were prepared as described previously [18] using rat anti-HA (1:500 dilution, Roche), mouse anti-GFP (1:500 dilution, Roche) and rabbit anti-CysRS (1:500 dilution) antibodies.

#### Generation of *E. coli* constructs and complementation experiments

The *Pf*CysRS gene, without the 75-amino-acid N-terminal apicoplast-targeting sequence, was synthesized as a codon-optimized sequence for protein expression in *E. coli* (Mr Gene). We investigated the aminoacylation activity of *Pf*CysRS by complementation of a temperature-sensitive mutant *cysRS E. coli* strain, UQ818 [44] (provided by The *E. coli* Genetic Stock Center, Yale University, New Haven, CT, U.S.A.). The recombinant codon-optimized *Pf*CysRS was subcloned into the pTrc99A plasmid (Pharmacia Biotech) with the restriction enzymes XbaI and SalI. Transformed UQ818 cells with empty pTrc99A and pTrc99A-*Pf*CysRS were streaked on to LB agar plates supplemented with ampicillin (100 $\mu$g/ml) and nalidixic acid (50 $\mu$g/ml). Transformants were incubated at the permissive temperature of 30 °C, and the non-permissive temperature of 42 °C, for 48 h. As a control, growth curves of DH5$\alpha$ cells transformed with pTrc99A and pTc99A-*Pf*CysRS were also analysed. Each strain was grown overnight in liquid culture (at 30 °C) and a $10^{-3}$ dilution was used to inoculate 20 ml of LB media supplemented with ampicillin (100 $\mu$g/ml) and nalidixic acid (50 $\mu$g/ml). Aliquots of 1 ml were taken every 30 min to measure the $D_{600}$ using a SmartSpec 3000 instrument (Bio-Rad Laboratories).

#### Generation of a CysRS expression vector, bacterial expression and purification

The synthetic *Pf*CysRS gene (see above) was designed to include the desired restriction sites and was subcloned into the final plasmid pET21a (Invitrogen). The pET21a-*Pf*CysRS clones were transformed into *E. coli* Rosetta 2 (DE3) pLysS cells. Transformants were grown in 1 litre of LB-ampicillin medium to a cell density ($D_{600}$) of 0.6. Protein expression was induced with 1 mM IPTG and incubation was carried out at 37 °C for 3 h. Cells were harvested and lysed with lysozyme (Sigma–Aldrich) in the presence of EDTA-free protease inhibitor cocktail (Roche). The cleared lysate was passed through a nickel-affinity column and recombinant *Pf*CysRS was purified according to the manufacturer's protocol (Novagen). The purified histidine-tagged *Pf*CysRS was judged to be of 95 % purity by SDS gel after Coomassie Brilliant Blue staining.

#### Preparation of tRNA transcripts

Transcripts of cytosolic and apicoplast *Plasmodium* $tRNA^{Cys}$ were prepared and purified as described previously [45]. The *P. falciparum* $tRNA^{Cys}$ transcript was synthesized with a 5′ extension that encoded a ribozyme to self-cleave the 5′ extension [46]. The cleavage reaction occurred during transcription and the processed tRNA lacking the 5′ extension was purified by extraction from a denaturing gel. [$^{35}$S]Cysteine was obtained from PerkinElmer. The tRNA transcripts were heat-denatured at 85 °C for 3 min and annealed at 37 °C for 20 min before use. These tRNAs, after denaturation by heat and annealing in the presence of 10 mM $Mg^{2+}$, exhibited a plateau level of aminoacylation of approximately 20 %. Steady-state aminoacylation assays were monitored at 37 °C in 20 mM Tris/HCl (pH 7.5), 20 mM KCl, 10 mM $MgCl_2$, 25 mM DTT, 50 $\mu$M cysteine and 2 mM ATP with 10–50 nM CysRS (depending on the activity towards different tRNAs) and varying tRNA concentrations (0.06–8 $\mu$M) to maintain steady-state conditions.

#### Assays for aminoacylation of tRNA with cysteine

The aminoacylation reaction was initiated by mixing the CysRS enzyme with various concentrations of an annealed tRNA transcript and [$^{35}$S]cysteine (specific activity of 5200–6600 d..p.m/pmol). The reaction mixture was aliquoted, quenched with the CAM solution [0.24 M iodoacetic acid and 0.1 M sodium acetate in formamide (pH 5.0)] [45], and was further incubated for 30 min at room temperature (22 °C). These samples were spotted on to filter papers and precipitated by 5 % TCA (trichloroacetic acid), and the unbound [$^{35}$S]cysteine was washed off from the paper pads. The concentration of aminoacylated tRNA at each time point was quantified by determining the radioactivity on each paper pad in a liquid scintillation counter (Beckman LS6000SC) and correcting for quenching effects. Steady-state kinetic parameters were determined by fitting initial aminoacylation rate against tRNA substrate concentration to the Michaelis–Menten equation.

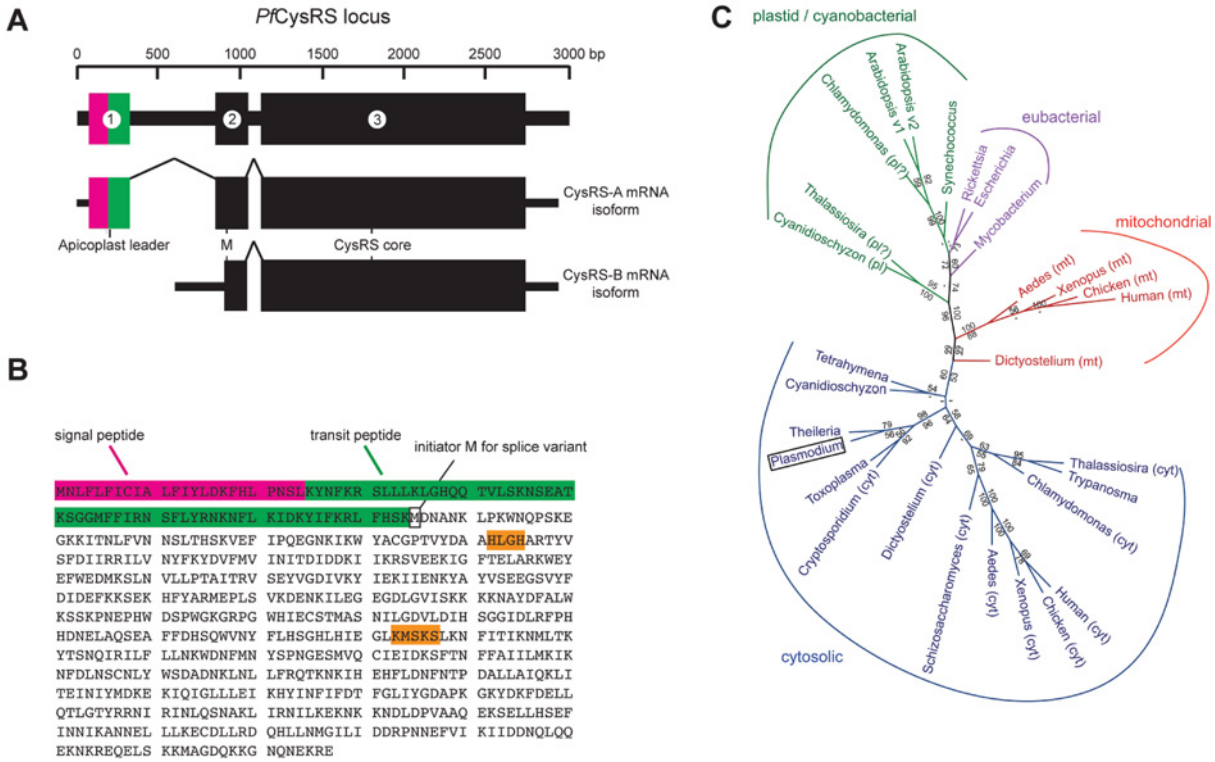


**Figure 1** ***Pf*CysRS exists as two isoforms and is alternatively spliced**

(**A**) Schematic diagram of the *Pf*CysRS gene locus and the two CysRS mRNA isoforms. The three exons are numbered, with exon 1 representing the apicoplast bipartite leader sequence. These exons are alternatively spliced to produce two transcript variants, one with and one without the apicoplast-targeting sequence. (**B**) The *Pf*CysRS protein sequence with the predicted signal sequence (magenta), transit peptide (green) and the signature HIGH and KMSKS motifs characteristic of class I aaRSs (orange). The internal methionine residue is outlined with a box. (**C**) Phylogenetic tree of select CysRSs constructed using a maximum-likelihood algorithm (PhyML). The tree shows that the single *Plasmodium* CysRS gene and the corresponding genes from the other related apicomplexans group with other cytosolic eukaryotic CysRS sequences (black) and not with mitochondrial (red) or plastid (green) CysRSs. The CysRSs of primary plastids, and some secondary plastids, group with cyanobacterial and other eubacterial sequences (purple). Bootstrap values are shown on branches and values below 50 are indicated by -. The eukaryotic isoforms are annotated: cyt, cytosolic isoforms; mt, mitochondrial isoforms; and pl, plastid isoforms.

## RESULTS AND DISCUSSION

### *P. falciparum* encodes a single eukaryotic-type CysRS

Bioinformatic analysis of the *P. falciparum* genome has revealed only a single copy of the CysRS gene (PF3D7_1015200.1) (Figure 1A). No other CysRS genes are encoded by either the apicoplast or the mitochondrial genomes [47]. Alignment of the amino acid sequence of this gene (hereafter called *Pf*CysRS) to other bacterial and eukaryotic CysRS sequences revealed an N-terminal extension, approximately 75 amino acid in length, not conserved in non-apicomplexan CysRSs. The characteristic KMSKS (Lys-Met-Ser-Lys-Ser) and HIGH (His-Ile-Gly-His) sequences for substrate binding [48] have been conserved in *Plasmodium* species. Unlike yeast and human CysRS [49], *Plasmodium* lacks the insertion domain found within the Rossmann fold (~100 amino acids). Interestingly, this insertion is not evenly distributed across all eukaryotes, but is well conserved in the opisthokonts. Previous analyses indicated that a C-terminal extension in the human CysRS, not found in bacteria, is involved in enhancing specificity for eukaryotic tRNA [50]. This extension is also found in *Plasmodium* and other apicomplexan CysRSs (Figure 1B).

Phylogenetic analysis of CysRSs shows a strong alliance between enzymes responsible for plastid aminoacylation and bacterial sequences (Figure 1C). This suggests a bacterial origin for plastid CysRS congruent with the primary endosymbiotic origin of the plastid. Trees inferred using multiple methods place the CysRSs from plant and green algal chloroplasts with cyanobacteria, the bacterial ancestor of plastids, albeit with bootstrap values consistently lower than 50. The plastid CysRS from the diatom *Thalassiosira* is grouped with the plastid CysRSs from a red alga (*Cyanidioschyzon*), consistent with the known red algal origin of the diatom plastid (Figure 1C). Mitochondrial CysRSs (with the exception of the slime mould *Dictyostelium*) form a distinct clade, although these sequences do not group with the $\alpha$-proteobacterial ancestors of mitochondria. Like bacterial sequences, mitochondrial and chloroplast CysRS sequences lack the C-terminal extension found in other eukaryotic CysRSs.

The *P. falciparum* CysRS forms a clade with other apicomplexan sequences, including the CysRS of *Cryptosporidium parvum,* which lacks an apicoplast and has no mitochondrial translation [51], so the *Cryptosporidium* CysRS must be a cytosolic enzyme. The apicomplexan clade is nested within the radiation of other cytosolic eukaryotic CysRSs. Together with the C-terminal eukaryote-specific extension, the phylogenetic analysis indicates a vertical eukaryotic (nuclear) ancestry for *Pf*CysRS, and no evidence for an origin by endosymbiotic gene transfer that is seen for the plastid CysRSs. Diatoms, relatives of the Apicomplexa, have two CysRSs: one that groups with the cytosolic eukaryotic sequences, and a second CysRS with a bipartite plastid-targeting leader, which groups strongly with the CysRS from a red alga (*Cyanidioschyzon*) related to the ancestor of diatoms' secondary endosymbiotic plastid (Figure 1C). A single secondary endosymbiosis is argued

to have given rise to the plastids of Chromalveolata, which includes diatoms and Apicomplexa [52], so the ancestor of Apicomplexa could originally have had a plastid-targeted CysRS derived from the red algal endosymbiont, as well as a cytosolic enzyme related to the cytosolic CysRSs of other eukaryotes. No mitochondrial CysRSs from any chromalveolate have been characterized, so their evolutionary origin and fate is unknown.

### *Pf*CysRS is alternatively spliced to produce forms with and without a bipartite apicoplast-targeting leader

The single *Pf*CysRS gene is annotated to contain three exons (Figure 1A), similar to the corresponding syntenic orthologues from all other annotated *Plasmodium* species. The initial exon consists almost entirely of coding sequence corresponding to a predicted bipartite apicoplast-targeting leader sequence with a signal peptide and transit peptide [29,53]. This predicted bipartite leader sequence stops at the start of the predicted second exon, at which point the protein sequence begins to exhibit a strong similarity to other CysRS sequences. This second exon also commences with a start codon with a preceding AAA nucleotide triplet characteristic of translation start sites in *Plasmodium*. RNA-Seq data from a whole genome analysis identifies a considerable pool of alternatively spliced transcripts that either lack all or part of the first exon, or which have an alternative splice event within the first intron. These alternative transcripts lack the complete open reading frame that commences with the methionine residue in the first annotated exon, and must therefore commence translation in the annotated second intron [54].

To confirm the existence of these alternatively spliced transcript forms we performed RT (reverse transcriptase)–PCR on mixed blood-stage *P. falciparum* parasites using a variety of different primer combinations to sequence the resulting cDNAs. Sequencing confirmed the existence of at least two transcript variants, one of which contained all three exons with the two introns spliced out as annotated in PlasmoDB v8.2 (GenBank® accession number KF056896), and the other (GenBank® accession number KF056897) showed only a single intron removed, whose open reading frame commenced with the start codon near the beginning of the annotated exon 2 (Figure 1A). These data confirm that this gene is alternatively spliced, producing alternative versions of the open reading frame, one commencing with the predicted bipartite apicoplast-targeting sequence, and the other lacking this putative trafficking information.

The exon structure of the CysRS gene is conserved between diverse *Plasmodium* species, and because all apicomplexans possess only a single CysRS protein and most possess an apicoplast, this suggests that similar alternative splicing is conserved throughout the genus. However, the gene structure is quite different in other apicomplexans, such as *Toxoplasma* and *Theileria*, so it is unclear if the mechanism of targeting via alternative splicing is shared for all apicomplexan CysRS enzymes.

### The bipartite leader sequence is sufficient for targeting GFP to the apicoplast in *P. falciparum*

To test whether the bioinformatically predicted bipartite apicoplast leader acts as a true apicoplast-targeting sequence, we tested whether this sequence was sufficient to target a reporter protein to the apicoplast. The first 153 amino acids of the protein sequence, consisting of the predicted bipartite leader, was cloned from *P. falciparum* cDNA, and fused in-frame in front of GFP in an overexpression plasmid (pGlux.1) controlled by the heterogeneous *Pf*CRT (CRT is chloroquine-resistance transporter) promoter. Parasites transfected with this construct (*Pf*CyRS-$A_{1–153}$GFP) were obtained approximately 26 days after transfection and were assayed by Western blotting and fluorescence microscopy. Live-cell imaging revealed the GFP signal for *Pf*CyRS-$A_{1–153}$GFP to be localized to a single organelle with morphology typical of apicoplast targeting (Figure 2A). Parasites had a single spherical punctum in early stages, which branched and divided in schizont stages before segregating into individual merozoites (results not shown). In immunofluorescence assays of *Pf*CyRS-$A_{1–153}$GFP, all of the GFP signal co-localized with a lumenal marker of the apicoplast, the ACP (Figure 2C). Western blot analysis confirmed overexpression of a protein of the expected mass for the fusion protein lacking the signal peptide and apicoplast transit peptide (Figure 2D). An additional form ~4 kDa larger was also observed after longer exposures (results not shown). These data are consistent with a model in which the reporter was imported to the apicoplast and the N-terminal extension removed in the apicoplast. This model is consistent with observations of nearly all native and exogenously apicoplast-targeted proteins (see, for example, [16,53]). These data confirmed targeting of this reporter (*Pf*CyRS-$A_{1–153}$GFP) to the apicoplast and confirm that the first exon of this gene is a true apicoplast-targeting leader sequence.

To test the targeting characteristics of protein commencing with the alternative translation start site, a GFP-fusion protein construct was also generated using an N-terminal fragment that started at the methionine residue located at the start of the annotated exon 2. A coding sequence corresponding to the 70 amino acids following this internal methionine residue was cloned from *P. falciparum* cDNA and this fragment was cloned into pGlux.1 as described above. Parasites were transfected and positive transfectants were established approximately 23 days later. Live-cell microscopy of this line (*Pf*CyRS-$B_{1–70}$GFP) demonstrated that this GFP-fusion protein was retained in the cytosol, with no apparent organellar accumulation (Figure 2B). These parasites were also assayed by Western blotting, which revealed tagging of a protein of the expected mass for the unprocessed protein fused to GFP (34.6 kDa). These data indicate that the internal alternative translation initiation site does not correspond to an organellar targeting sequence, consistent with the observation that protein initiating from this site is retained in the cytosol.

### Endogenous *Pf*CysRS tagged with a HA epitope is targeted to the cytosol and apicoplast: a model of dual targeting

Despite the use of the deliberately weak *Pf*CRT promoter, episomally expressed transgenes in the pGlux.1 expression system may not faithfully reflect native protein localization. Such episomal transfectants also lack chromosomal context that may be necessary to recapitulate true splicing events. Subcellular localization of the native *Pf*CysRS was further studied using an affinity-purified rabbit antibody raised against a peptide from *Pf*CysRS. Immunofluorescence assays using these antisera also showed that the major fraction of the *Pf*CysRS was localized in the cytosol, but also identified a further minor fraction in the apicoplast (Figure 3A). Western blot analysis showed specific recognition of the ~69 kDa protein, consistent with the predicted mass of both the cytosolic protein and the truncated apicoplast protein (Figure 3B).

We also followed the targeting of the endogenous copy of *Pf*CysRS by introducing the sequence of a triple haemagluttinin tag (3×HA) into the 3′ end of the gene using the pHA3 recombination vector. Parasites were recovered after 15 days, then subsequently cycled on and off selective agent (WR99210) to select for parasites that had integrated the plasmid into the

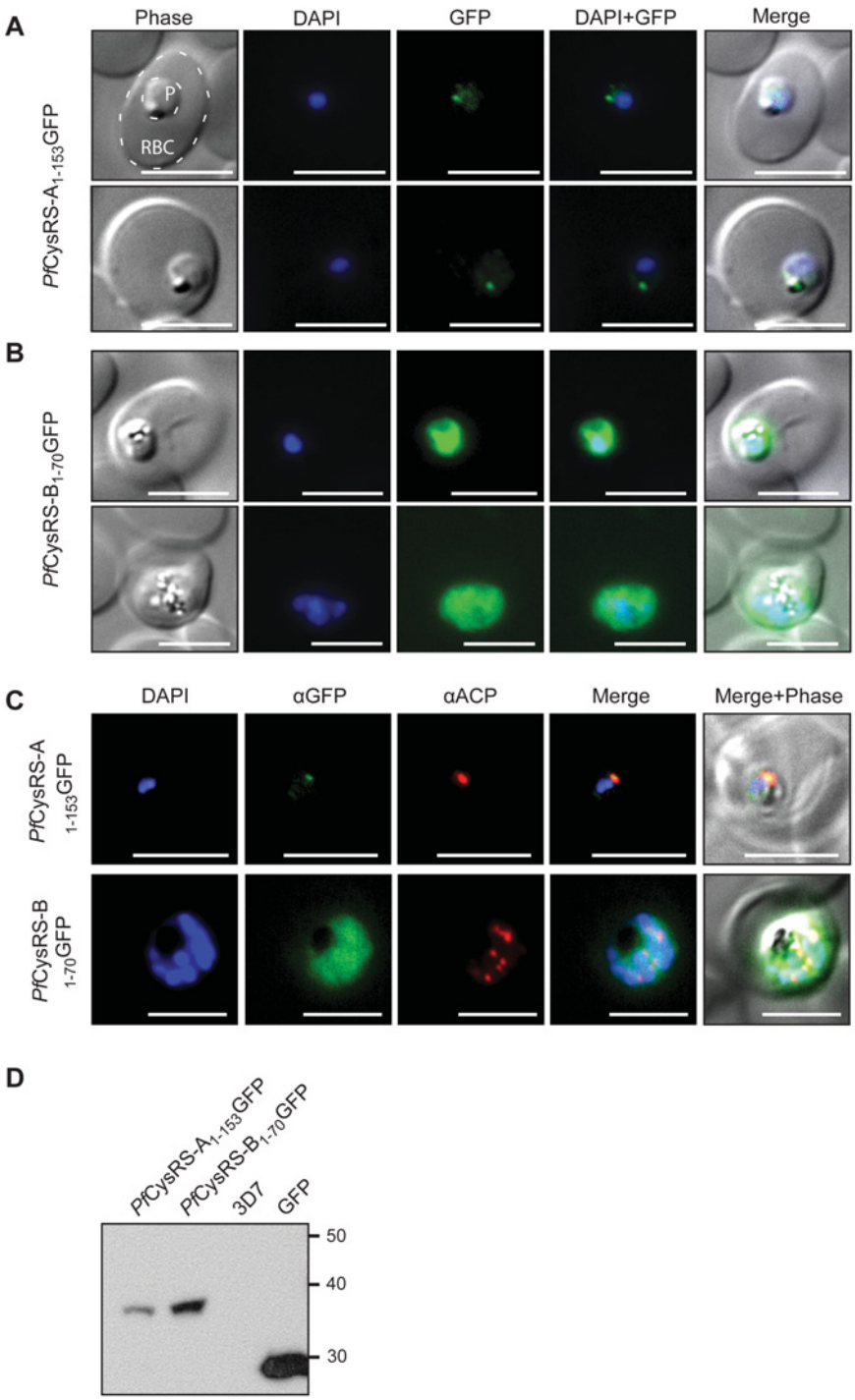


**Figure 2 Localization of *Pf*CysRS isoforms using GFP fusions in transgenic *Plasmodium* parasites**

Live-cell epifluorescence microscopy of *P. falciparum* transfected using pGlux.1 vector for episomal expression of GFP fused to the two *Pf*CysRS mRNA isoforms: *Pf*CysRS-$A_{1–153}$GFP (**A**) and *Pf*CysRS-$B_{1–70}$GFP (**B**) in live cells. In (**A**), both parasites are early trophozoite stage, and localization of GFP is to a single punctum, consistent with the size and position of the apicoplast. The red blood cell (RBC) and the parasite (P) are indicated. (**B**) An early trophozoite (top panels) and late trophozoite (bottom panels) with GFP dispersed throughout the cytosol. (**C**) Immunofluorescence assays of the parasites indicated, *Pf*CysRS-$A_{1–153}$GFP (top panels) and *Pf*CysRS-$B_{1–70}$GFP (bottom panels), using antibodies against GFP and ACP, an apicoplast marker. The *Pf*CysRS-$A_{1–153}$GFP signal specifically co-localizes with the apicoplast marker, whereas the *Pf*CysRS-$B_{1–70}$GFP signal is distributed throughout the cytosol. For (**A**)–(**C**), all scale bars indicate 5 $\mu$m. (**D**) Western blot analysis of the transfectants indicated using an anti-GFP antibody. The two *Pf*CysRS–GFP fusions ran at their expected molecular mass, with *Pf*CysRS-$A_{1–153}$GFP in the mature processed form having the signal peptide and transit peptide cleaved off. The 3D7 parasite strain was used as a negative control and purified recombinant GFP was used as a positive control. The molecular mass in kDa is indicated on the right-hand side.

*Pf*CysRS locus. Stable transgenic integrants were obtained after the third cycle and were assessed by Western blot analysis and immunofluorescence assays. Western blot analysis revealed that the HA tag had integrated into the expected gene, producing a band at ~72 kDa (Figure 3B). This is congruent with a protein with translation initiation at the internal methionine residue with the

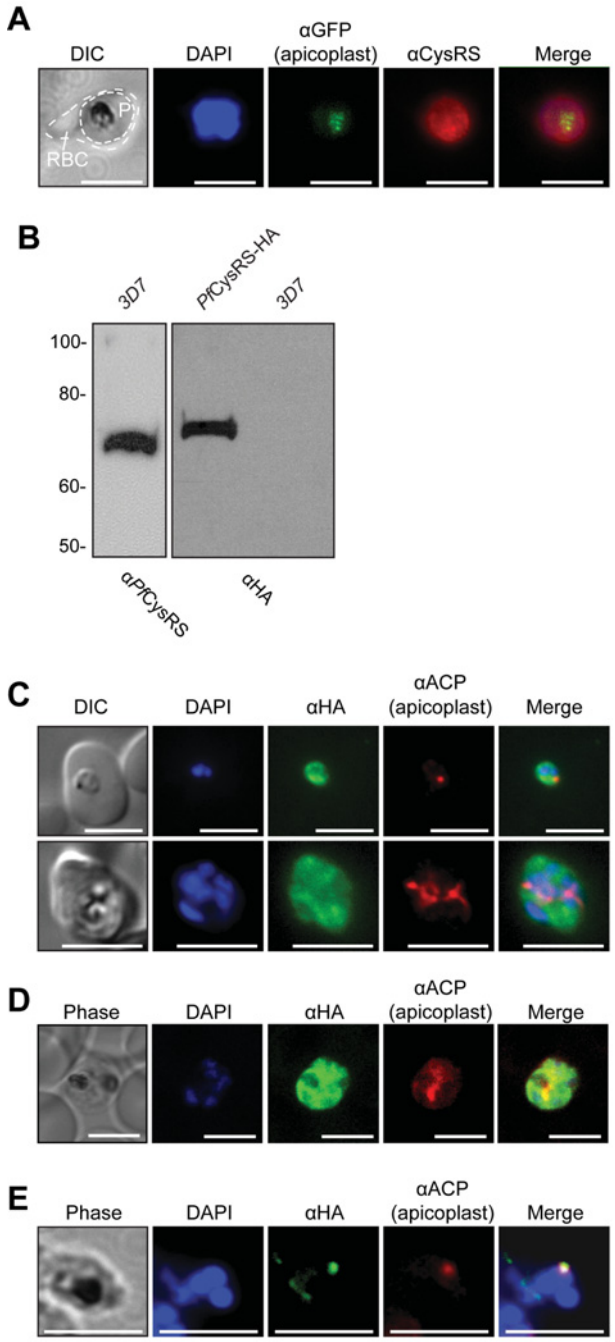


**Figure 3 Co-localization of CysRS by immunofluorescence assays in *P. falciparum***

(**A**) Immunofluorescence assays of trophozoite stage *P. falciparum* (3D7 strain) using an anti-*Pf*CysRS antibody, DAPI and the apicoplast marker PfRRf1–GFP. The red blood cell is indicated (RBC) and the parasite is indicated (P). (**B**) Western blot analysis showing *Pf*CysRS at the expected molecular mass of ∼69 kDa in the 3D7 strain using an anti-CysRS antibody (left-hand panel). *Plasmodium* parasites transfected and selected for integration of a 3′ HA tag at the endogenous locus were probed with an anti-HA antibody (right-hand panel) with an expected molecular mass of ∼72 kDa. The 3D7 strain served as a negative control. (**C**) Epifluoresence microscopy and (**D**) confocal imaging of immunofluorescence analysis of *Pf*CysRS–HA transfectants at early- and late-trophozoite stage parasites (top and bottom panels respectively) with an anti-HA antibody against the *Pf*CysRS–HA enzyme, an anti-ACP antibody for the apicoplast, and DAPI for the nucleus. The images show that the *Pf*CysRS–HA is distributed throughout the cytosol, and also overlap with the apicoplast marker ACP. The width of the apicoplast is less than the spatial resolution of light microscopy, so we cannot definitively assign co-localization from these experiments. (**D**) Confocal images of *Pf*CysRS–HA transfectant parasites at late-trophozoite stage using indirect immunofluorescence analysis reveals cytoplasmic distribution of *Pf*CysRS–HA overlapping with the apicoplast marker ACP. (**E**) Immunofluorescence analysis with saponin-treated *Pf*CysRS–HA to differentially lyse membranes to allow for visualizing subcellular organelles with antibodies and stains as indicated. Parasites are labelled with an anti-HA antibody against the *Pf*CysRS–HA enzyme, and an anti-ACP antibody as a marker of the apicoplast. This immunolocalization confirms that a fraction of *Pf*CysRS is specifically retained within the apicoplast. All scale bars indicate 5 $\mu$m.

added 3×HA tag (73 kDa). However, this would also be consistent with a processed product that initiated at the first methionine residue and had the bipartite apicoplast leader removed, which could be between ∼72 and 76 kDa.

The *Pf*CysRS–HA-tagged parasites were used to perform immunofluorescence assays, which revealed that most of the protein was localized to the parasite cytosol, whereas some *Pf*CysRS–HA co-localized with the ACP apicoplast marker (Figure 3C). However, because of the strong cytosolic background labelling of the *Pf*CysRS–HA, and the small diameter of the apicoplast (∼200 nm), it was difficult to be sure that this was not fluorescence from protein just outside of the apicoplast. Analysis of labelling using confocal microscopy (Figure 3D) and image deconvolution (Supplementary Movie S1 at http://www.biochemj.org/bj/458/bj4580513add.htm) were congruent with co-localization, but did not prove this explicitly. We addressed this uncertainty in apicoplast localization through a differential permeabilization approach previously used for apicoplast labelling [18]. This demonstrated that when the cytosolic fraction of *Pf*CysRS–HA was extracted, a specific punctum remained, co-localized with the apicoplast marker ACP. The results indicate that for this tagged native gene product, a major isoform exists in the parasite cytosol, but a minor isoform also exists in the apicoplast lumen (Figure 3E). No such apicoplast fraction remained using the GFP-tagged truncated cytosolic isoform (results not shown).

The single *Tg*CysRS has previously been investigated using reporter genes not in the native genomic context and using exogenous promoters [20]. We investigated trafficking of this protein from the endogenous locus to more faithfully recapitulate native splicing and expression of the gene. We introduced a 3×HA tag into the 3′ terminus of the single chromosomal *Tg*CysRS gene in a ΔKU80 *T. gondii* strain. Only a single protein species was present at ∼75 kDa (Supplementary Figure S1A at http://www.biochemj.org/bj/458/bj4580513add.htm). This is smaller than the predicted mass from the gene model based on RNA-Seq data (∼90 kDa) and our sequence of cDNA obtained derived from a 5′ RACE pool (GenBank® accession number KF056898). This discrepancy suggests translation from an internal methionine residue or alternative splicing as for the *Plasmodium* orthologue, although we found no alternative transcripts by 5′ RACE. We attempted to perform solubilization on these transfectants to further investigate the apicoplast isoform, but were unable to find any conditions that gave clean differentiation between plastid and cytosolic fractions [55,56]. Immunolocalization of this HA-tagged *Tg*CysRS showed a similar pattern to the *Plasmodium* orthologue, with a dominant cytosolic localization, as well as some signal overlapping with the Cpn60 apicoplast marker [57] (Supplementary Figure S1B), although the small size of the organelle means that we cannot distinguish whether this overlap is specific apicoplast localization, or spatially unresolved fluorescence from the surrounding cytosol.

Taken together, the results of the present study show that the *Pf*CysRS is alternatively spliced to produce isoforms that are respectively targeted to the apicoplast and cytosol. Targeting of individual proteins to multiple organelles has also been observed for several other *P. falciparum* proteins [18,58,59], although a molecular mechanism for targeting to multiple destinations has not been directly demonstrated in any of these cases.

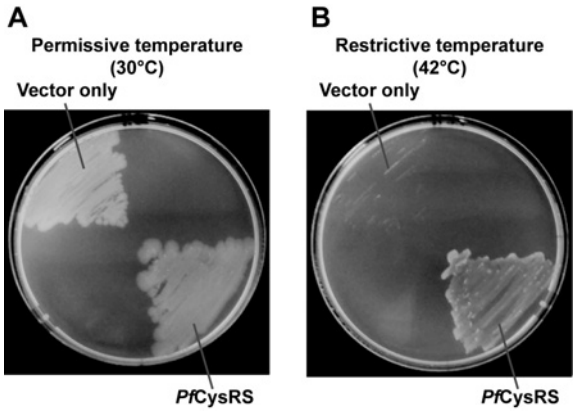


**Figure 4 Complementation of a temperature-sensitive *cysRS E. coli* strain with *Pf*CysRS**

The temperature-sensitive *cysRS E. coli* strain UQ818 was transformed with the pTrc99a vector containing *Pf*CysRS (truncated to remove the apicoplast-targeting sequence), and empty vector as a control. Both transformants were streaked on to LB agar plates supplemented with ampicillin (100 $\mu$g/ml) and nalidixic acid (50 $\mu$g/ml) then grown for 48 h at the permissive (**A**) and restrictive (**B**) temperatures, 30 °C and 42 °C respectively. Bacteria only grew at the restrictive temperature when they were transformed with a vector expressing *Pf*CysRS, indicating that this enzyme complements the *cysRS* defect in UQ818 *E. coli*.

### *Pf*CysRS complements an *E. coli cysRS* temperature-sensitive mutant

The *E. coli* K-12 strain UQ818 is a temperature-sensitive mutant isolated as a spontaneous mutant that lacks CysRS activity above the permissive temperature of 40 °C [44]. The CysRS activity in this mutant is defective at non-permissive temperatures due to a single amino acid change (V27E) that disrupts cysteine binding [60]. A truncated version of the *Pf*CysRS lacking the apicoplast-targeting sequence was expressed in UQ818 and tested for growth in both liquid and solid media. The UQ818 mutant transformed with empty pTrc99a vector was able to grow at the permissive temperature of 37 °C (Figure 4A), but showed no growth at 42 °C (Figure 4B). The *Pf*CysRS-containing vector restored growth at the restrictive 42 °C on solid media (Figure 4B) and in liquid media (results not shown). Expression in a CysRS-wt (wild-type) DH5$\alpha$ strain revealed no growth differences. Complementation of the *cysRS* defect in UQ818 demonstrates that the *Pf*CysRS has aminoacylation activity and is able to recognize *E. coli* tRNA$^{Cys}$.

### Analysis of the cytosolic and apicoplast *P. falciparum* tRNA$^{Cys}$ molecules

Sequence analysis of *P. falciparum* tRNA$^{Cys}$ revealed that although the cytosolic version possesses all of the canonical features as in *E. coli* tRNA$^{Cys}$ (Figure 5A), the apicoplast version possesses unusual features (Figure 5B). Although all three tRNAs contain U73 as the discriminator base and the 5′-GCA sequence as the anticodon, which are major determinants for aminoacylation with cysteine [50], the apicoplast tRNA$^{Cys}$ is distinct in the following ways. First, it has A1–U72 and A2–U71 as the first two base pairs in the acceptor stem, which differ from the canonical G1–C72 and G2–C71 base pairs (Figure 5B). The higher A–U content in the acceptor end may confer unusual conformations to the CCA terminus [61]. Secondly, it has an A15–U48 tertiary base pair, in contrast with the more common G15–C48 base pair as in the cytosolic version (Figure 5B). Interestingly, *E. coli* tRNA$^{Cys}$ has an unusual G15–G48 base pair (Figure 5C), which modulates the activity of aminoacylation [45,62]. Thirdly, the apicoplast tRNA$^{Cys}$ contains A19, rather than the conserved G19, in the D loop that forms a tertiary base pair with C56 in the T loop in the canonical structure (Figure 5B). The possession of A19 may permit the formation of a novel A19–U56 base pair in the apicoplast form. Other unusual features of the apicoplast tRNA$^{Cys}$ are the anticodon stem, made up of entirely A–U base pairs, and the use of an A30–U40 base pair in the anticodon stem, in contrast with the more common G30–C40 sequence.

### Enzyme kinetics of *P. falciparum* CysRS

To evaluate the activity of *Pf*CysRS for aminoacylation of the cytosolic and apicoplast versions of tRNA$^{Cys}$, we carried out steady-state kinetics analysis using purified recombinant *Pf*CysRS enzyme and tRNA transcripts. The aminoacylation activity for each tRNA was examined by steady-state kinetic analysis under conditions where tRNA was in excess of the enzyme so the synthesis of cysteinyl-tRNA$^{Cys}$ was linear with time (Supplementary Figure S2). Each tRNA transcript was prepared by transcription using T7 RNA polymerase and heat-cooled

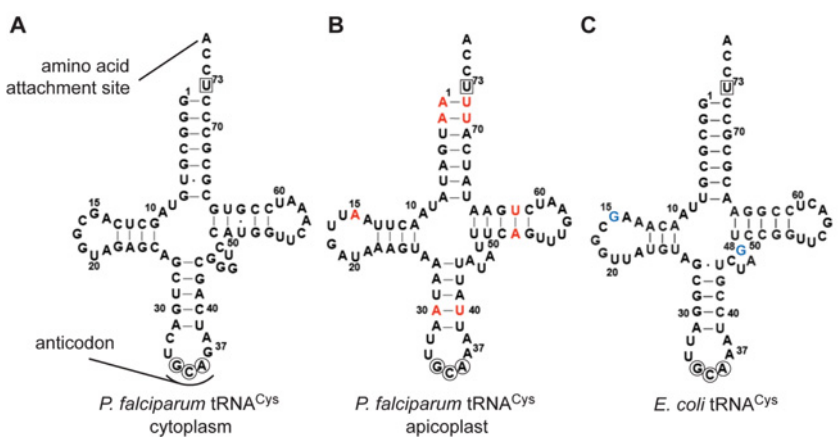


**Figure 5 Cloverleaf structures of tRNA$^{Cys}$**

Structures and sequence for *P. falciparum* cytosolic tRNA$^{Cys}$ (**A**), *P. falciparum* apicoplast tRNA$^{Cys}$ (**B**) and *E. coli* tRNA$^{Cys}$ (**C**). Specific features of the tRNA are indicated: the ACG anticodon is circled and the U73 stem discriminator is boxed. For the apicoplast tRNA$^{Cys}$, the bases not found in either the cytosolic tRNA$^{Cys}$ or *E. coli* tRNA$^{Cys}$ are highlighted in red. The G15–G48 Levitt pair found in the *E. coli* tRNA$^{Cys}$ is shown in blue. The anticodon loop and the amino acid attachment site are indicated.

**Table 1 Summary of the steady-state kinetic parameters for synthesis of cysteine-tRNA$^{Cys}$ by aminoacylation with cysteine to *P. falciparum* cytosolic and apicoplast tRNA$^{Cys}$ and *E. coli* tRNA$^{Cys}$ by the respective CysRS enzymes**

(a) *Pf*CysRS

| tRNA$^{Cys}$ | $K_m$ (tRNA) ($\mu$M) | $k_{cat}$ ($s^{-1}$) | $K_{cat}/K_m$ ($\mu M^{-1} \cdot s^{-1}$) | Ratio |
|---|---|---|---|---|
| *P. falciparum* tRNA$^{Cys}$, cytosolic | $0.25 \pm 0.05$ | $0.24 \pm 0.01$ | $0.96 \pm 0.29$ | 1.0 |
| *P. falciparum* tRNA$^{Cys}$, apicoplast | $1.45 \pm 0.13$ | $0.086 \pm 0.003$ | $0.060 \pm 0.005$ | 1:16 |
| *E. coli* tRNA$^{Cys}$ | $0.65 \pm 0.15$ | $0.19 \pm 0.01$ | $0.28 \pm 0.04$ | 1:3.4 |

(b) *E. coli* CysRS

| | $K_m$ (tRNA) ($\mu$M) | $k_{cat}$ ($s^{-1}$) | $K_{cat}/K_m$ ($\mu M^{-1} \cdot s^{-1}$) | Ratio |
|---|---|---|---|---|
| *E. coli* tRNA$^{Cys}$ | $1.2 \pm 0.01$ | $1.2 \pm 0.07$ | $1.1 \pm 0.07$ | 1:3.9 |

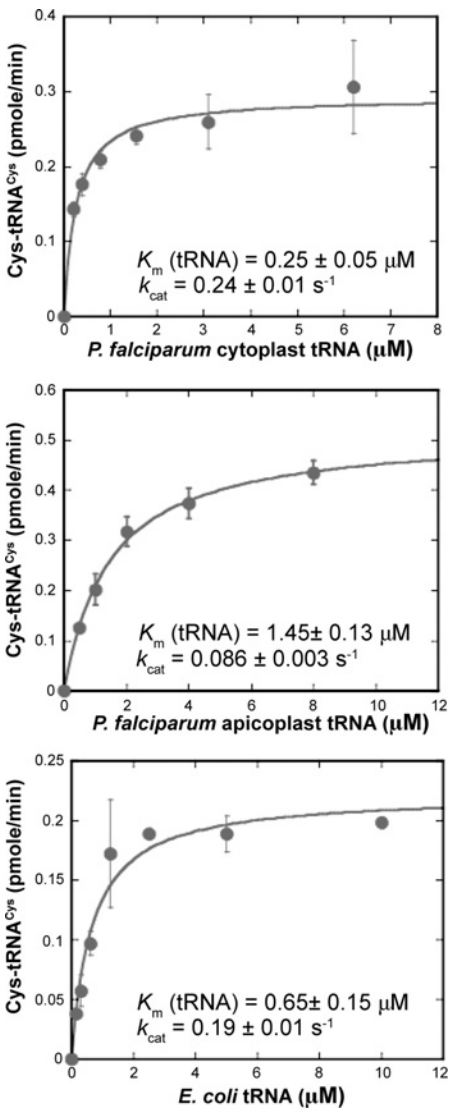


**Figure 6 Steady-state kinetic parameters of *Plasmodium* and *E. coli* tRNA$^{Cys}$**

Aminoacylation assays with saturating [$^{35}$S]cysteine, at various concentrations of tRNA$^{Cys}$. Steady-state kinetic parameters were determined by fitting initial aminoacylation rates against tRNA substrate concentrations to the Michaelis–Menten equation.

annealed to serve as the substrate for aminoacylation. Plateau levels of aminoacylation for cytosolic and apicoplast tRNA$^{Cys}$ were at 19 and 11 % in extended time courses respectively. We also tested *E. coli* tRNA$^{Cys}$, which has been well characterized [4,63,65], as a substrate for comparison.

The $k_{cat}$ and $K_m$ (tRNA) values for each tRNA were measured from fitting the data of the initial rate of aminoacylation as a function of tRNA concentration to the Michaelis–Menten equation (Figure 6). These data are summarized in Table 1. The $K_m$ (tRNA, $0.25 \pm 0.05$ $\mu$M), $k_{cat}$ ($0.24 \pm 0.01$ $s^{-1}$) and $k_{cat}/K_m$ ($0.96 \pm 0.6$ $\mu M^{-1} \cdot s^{-1}$) values of the *Pf*CysRS enzyme for the cytosolic tRNA were closely similar to known values of CysRS, where $K_m$ is typically $\sim 1$ $\mu$M, $k_{cat}$ is $\sim 1$ $s^{-1}$ and $k_{cat}/K_m$ is $\sim 1$ $\mu M^{-1} \cdot s^{-1}$ [50], indicating that the recombinant enzyme was active and that it exhibited a normal activity with the cytosolic tRNA. The recombinant enzyme also efficiently aminoacylated the transcript of *E. coli* tRNA$^{Cys}$, with kinetic parameters equivalent to those of the cytosolic tRNA, but with an overall 3.4-fold decrease in the catalytic efficiency of aminoacylation $k_{cat}/K_m$. This indicates that the *Pf*CysRS enzyme is similar to eukaryotic enzymes (e.g. human CysRS), which readily accommodate *E. coli* tRNA$^{Cys}$ [50,66,67]. The quality of transcription was verified using *E. coli* CysRS as a control to show that aminoacylation of *E. coli* tRNA$^{Cys}$ by the homologous *E. coli* enzyme exhibited normal kinetic parameters (Table 1).

Interestingly, aminoacylation of the apicoplast tRNA$^{Cys}$ by *Pf*CysRS was less efficient by 16-fold as compared with the cytosolic tRNA (Table 1). The defect was found in both the $K_m$ for tRNA, showing an increase to $1.45 \pm 0.13$ $\mu$M, and the $k_{cat}$ of aminoacylation, showing a decrease to $0.086 \pm 0.003$ $s^{-1}$, with an overall decrease in $k_{cat}/K_m$ to $0.06 \pm 0.005$ $\mu M^{-1} \cdot s^{-1}$.

Together, these aminoacylation activity results confirm that the *Pf*CysRS is able to recognize and charge the tRNA$^{Cys}$ molecules encoded by the nucleus and the apicoplast. Although the cytosolic tRNA$^{Cys}$ is efficiently recognized by *Pf*CysRS (Figure 5 and Table 1), the apicoplast tRNA$^{Cys}$ is recognized less efficiently (Table 1). The discrimination in aminoacylation of the apicoplast tRNA by *Pf*CysRS may reflect the presence of unusual features in the apicoplast tRNA, or the decreased aminoacylation activity could be related to unknown base modifications that may exist in the apicoplast tRNA and are not recapitulated in our heterologous transcription system. We note that the apicoplast encodes a mere 30 proteins in comparison with over 5000 by the nucleus. Furthermore, apicoplast-encoded proteins are translated in modest amounts; none are readily detectable without resorting to $^{14}C/^{35}S$ amino acid labelling [68,69]. The requirements for tRNA charging and turnover in the apicoplast, although absolute, are therefore likely to be very minimal, such that a *Pf*CysRS with weak activity for the apicoplast tRNA might suffice.

## Conclusions

In the present study we show that *Pf* CysRS mRNA is alternatively spliced, producing transcript versions with and without apicoplast trafficking sequences, resulting in accumulation of protein in both the apicoplast and the cytosol (Figures 2 and 3). This produces enzymes that recognize and charge both nuclear and apicoplast $tRNA^{Cys}$. The presence of an aaRS that is likely to be essential for translation in all compartments of *Plasmodium* presents an attractive drug target. aaRSs are being keenly pursued as drug targets in many organisms, with several compounds shown to be selective inhibitors targeting aaRSs in *Plasmodium* [70–72]. Inhibition of *Plasmodium* CysRS would probably have similar actions as borrelidin, an inhibitor of the dual-targeted *Plasmodium* threonyl-tRNA synthetase, which leads to widespread translational arrest and death [18,73]. In contrast, antimalarial drugs that affect apicoplast housekeeping processes often result in a 'delayed death' phenomenon whereby parasites die only in the subsequent proliferative cycle after drug treatment [74,75]. It is conceivable that compounds inhibiting both apicoplast and cytosolic translation may have a double effect, killing some parasites through inhibition of cytosolic translation, but additionally disrupting the apicoplast so that escapees of the first effect do not proliferate. This dual action may therefore act to slow drug resistance. Given these qualities, inhibitors of the dual-targeted CysRS should possess rapid antimalarial activity, thereby combining the advantages of rapid parasite death with a delayed disruption of organellar division and segregation that could 'mop up' survivors of the first mode of action.

## AUTHOR CONTRIBUTION

James Pham, Reiko Sakaguchi, Nilushi De Silva, Lee Yeoh and Stuart Ralph designed and performed experiments, analysed data and wrote the paper. Ya-Ming Hou and Geoffrey McFadden designed experiments, analysed data and wrote the paper.

## ACKNOWLEDGEMENTS

We thank Giel G. van Dooren (Research School of Biology, Australian National University, Canberra, Australia) for his reagents and helpful discussions. The Australian Red Cross Blood Service kindly supplied blood.

## FUNDING

This work was supported by the Australian Research Council [grant numbers FT0990350, DP130103236], the Australian NHMRC (National Health and Medical Research Council) [grant numbers 520700, 628704 and 637406 (to S.A.R.)] and an NHMRC program grant (to G.I.M.). J.S.P. and L.M.Y. are supported by Australian Postgraduate Awards. The research stay of J.S.P. with the Hou laboratory at Thomas Jefferson University, Philadelphia, PA, U.S.A. was supported by a J.D. Smyth Postgraduate Student Travel Award from The Australian Society for Parasitology.

## REFERENCES

1 Ambrogelly, A., Ahel, I., Polycarpo, C., Bunjun-Srihari, S., Krett, B., Jacquin-Becker, C., Ruan, B., Kohrer, C., Stathopoulos, C., RajBhandary, U. L. and Soll, D. (2002) *Methanocaldococcus jannaschii* prolyl-tRNA synthetase charges tRNA(Pro) with cysteine. J. Biol. Chem. **277**, 34749–34754

2 Ibba, M. and Soll, D. (2001) The renaissance of aminoacyl-tRNA synthesis. EMBO Rep. **2**, 382–387

3 Hauenstein, S., Zhang, C.-M., Hou, Y.-M. and Perona, J. J. (2004) Shape-selective RNA recognition by cysteinyl-tRNA synthetase. Nat. Struct. Mol. Biol. **11**, 1134–1141

4 Zhang, C.-M., Christian, T., Newberry, K. J., Perona, J. J. and Hou, Y.-M. (2003) Zinc-mediated amino acid discrimination in cysteinyl-tRNA synthetase. J. Mol. Biol. **327**, 911–917

5 Ibba, M., Hong, K. W., Sherman, J. M., Sever, S. and Soll, D. (1996) Interactions between tRNA identity nucleotides and their recognition sites in glutaminyl-tRNA synthetase determine the cognate amino acid affinity of the enzyme. Proc. Natl. Acad. Sci. U.S.A. **93**, 6953–6958

6 Jeannin, G., Burkard, G. and Weil, J. H. (1976) Aminoacylation of *Phaseolus vulgaris* cytoplasmic, chloroplastic and mitochondrial tRNAsPro and tRNAsLys by homologous and heterologous enzymes. Biochim. Biophys. Acta **442**, 24–31

7 Duchene, A.-M., Giritch, A., Hoffmann, B., Cognat, V., Lancelin, D., Peeters, N. M., Zaepfel, M., Marechal-Drouard, L. and Small, I. D. (2005) Dual targeting is the rule for organellar aminoacyl-tRNA synthetases in *Arabidopsis thaliana*. Proc. Natl. Acad. Sci. U.S.A. **102**, 16484–16489

8 Small, I., Wintz, H., Akashi, K. and Mireau, H. (1998) Two birds with one stone: genes that encode products targeted to two or more compartments. Plant Mol. Biol. **38**, 265–277

9 Rettig, J., Wang, Y., Schneider, A. and Ochsenreiter, T. (2012) Dual targeting of isoleucyl-tRNA synthetase in *Trypanosoma brucei* is mediated through alternative trans-splicing. Nucleic Acids Res. **40**, 1299–1306

10 Rinehart, J., Krett, B., Rubio, M. A., Alfonzo, J. D. and Soll, D. (2005) *Saccharomyces cerevisiae* imports the cytosolic pathway for Gln-tRNA synthesis into the mitochondrion. Genes Dev. **19**, 583–592

11 Dias, J., Octobre, G., Kobbi, L., Comisso, M., Flisiak, S. and Mirande, M. (2012) Activation of human mitochondrial lysyl-tRNA synthetase upon maturation of its premitochondrial precursor. Biochemistry **51**, 909–916

12 Morgante, C. V., Rodrigues, R. A., Marbach, P. A., Borgonovi, C. M., Moura, D. S. and Silva-Filho, M. C. (2009) Conservation of dual-targeted proteins in *Arabidopsis* and rice points to a similar pattern of gene-family evolution. Mol. Genet. Genomics **281**, 525–538

13 McFadden, G. I., Reith, M. E., Munholland, J. and Lang-Unnasch, N. (1996) Plastid in human parasites. Nature **381**, 482–482

14 Bhatt, T. K., Kapil, C., Khan, S., Jairajpuri, M. A., Sharma, V., Santoni, D., Silvestrini, F., Pizzi, E. and Sharma, A. (2009) A genomic glimpse of aminoacyl-tRNA synthetases in malaria parasite *Plasmodium falciparum*. BMC Genomics **10**, 644

15 Jackson, K. E., Habib, S., Frugier, M., Hoen, R., Khan, S., Pham, J. S., Ribas de Pouplana, L., Royo, M., Santos, M. A., Sharma, A. and Ralph, S. A. (2011) Protein translation in *Plasmodium* parasites. Trends Parasitol. **27**, 467–476

16 Waller, R. F., Reed, M. B., Cowman, A. F. and McFadden, G. I. (2000) Protein trafficking to the plastid of *Plasmodium falciparum* is via the secretory pathway. EMBO J. **19**, 1794–1802

17 Motorin, Y. and Waller, J. P. (1998) Purification and properties of cysteinyl-tRNA synthetase from rabbit liver. Biochimie **80**, 579–590

18 Jackson, K. E., Pham, J. S., Kwek, M., De Silva, N. S., Allen, S. M., Goodman, C. D., McFadden, G. I., de Pouplana, L. R. and Ralph, S. A. (2012) Dual targeting of aminoacyl-tRNA synthetases to the apicoplast and cytosol in *Plasmodium falciparum*. Int. J. Parasitol. **42**, 177–186

19 Khan, S., Sharma, A., Jamwal, A., Sharma, V., Pole, A. K. and Thakur, K. K. (2011) Uneven spread of cis- and trans-editing aminoacyl-tRNA synthetase domains within translational compartments of *P. falciparum*. Sci. Rep. **1**, 188

20 Pino, P., Aeby, E., Foth, B. J., Sheiner, L., Soldati, T., Schneider, A. and Soldati-Favre, D. (2010) Mitochondrial translation in absence of local tRNA aminoacylation and methionyl tRNAMet formylation in Apicomplexa. Mol. Microbiol. **76**, 706–718

21 Istvan, E. S., Dharia, N. V., Bopp, S. E., Gluzman, I., Winzeler, E. A. and Goldberg, D. E. (2011) Validation of isoleucine utilization targets in *Plasmodium falciparum*. Proc. Natl. Acad. Sci. U.S.A. **108**, 1627–1632

22 Ishiyama, A., Iwatsuki, M., Namatame, M., Nishihara-Tsukashima, A., Sunazuka, T., Takahashi, Y., Omura, S. and Otoguro, K. (2011) Borrelidin, a potent antimalarial: stage-specific inhibition profile of synchronized cultures of *Plasmodium falciparum*. J. Antibiot. (Tokyo) **64**, 381–384

23 Aurrecoechea, C., Brestelli, J., Brunk, B. P., Dommer, J., Fischer, S., Gajria, B., Gao, X., Gingle, A., Grant, G., Harb, O. S. et al. (2009) PlasmoDB: a functional genomic database for malaria parasites. Nucleic Acids Res. **37**, D539–D543

24 Altschul, S. F., Madden, T. L., Schaffer, A. A., Zhang, J., Zhang, Z., Miller, W. and Lipman, D. J. (1997) Gapped BLAST and PSI-BLAST: a new generation of protein database search programs. Nucleic Acids Res. **25**, 3389–3402

25 Benson, D. A., Karsch-Mizrachi, I., Lipman, D. J., Ostell, J. and Sayers, E. W. (2011) GenBank. Nucleic Acids Res. **39**, D32–D37

26 Chen, F., Mackey, A. J., Stoeckert, Jr, C. J. and Roos, D. S. (2006) OrthoMCL-DB: querying a comprehensive multi-species collection of ortholog groups. Nucleic Acids Res. **34**, D363–D368

27 Petersen, T. N., Brunak, S., von Heijne, G. and Nielsen, H. (2011) SignalP 4.0: discriminating signal peptides from transmembrane regions. Nat. Methods **8**, 785–786

28 Zuegge, J., Ralph, S., Schmuker, M., McFadden, G. I. and Schneider, G. (2001) Deciphering apicoplast targeting signals: feature extraction from nuclear-encoded precursors of *Plasmodium falciparum* apicoplast proteins. Gene **280**, 19–26

29 Foth, B., Ralph, S., Tonkin, C., Struck, N., Fraunholz, M., Roos, D., Cowman, A. and McFadden, G. (2003) Dissecting apicoplast targeting in the malaria parasite *Plasmodium falciparum*. Science **299**, 705–708

30 Felsenstein, K. M. and Lewis-Higgins, L. (1993) Processing of the $\beta$-amyloid precursor protein carrying the familial, Dutch-type, and a novel recombinant C-terminal mutation. Neurosci. Lett. **152**, 185–189
31 Neron, B., Menager, H., Maufrais, C., Joly, N., Maupetit, J., Letort, S., Carrere, S., Tuffery, P. and Letondal, C. (2009) Mobyle: a new full web bioinformatics framework. Bioinformatics **25**, 3005–3011
32 Guindon, S., Dufayard, J. F., Lefort, V., Anisimova, M., Hordijk, W. and Gascuel, O. (2010) New algorithms and methods to estimate maximum-likelihood phylogenies: assessing the performance of PhyML 3.0. Syst. Biol. **59**, 307–321
33 Kyes, S., Pinches, R. and Newbold, C. (2000) A simple RNA analysis method shows var and rif multigene family expression patterns in *Plasmodium falciparum*. Mol. Biochem. Parasitol. **105**, 311–315
34 Boddey, J. A., Moritz, R. L., Simpson, R. J. and Cowman, A. F. (2009) Role of the *Plasmodium* export element in trafficking parasite proteins to the infected erythrocyte. Traffic **10**, 285–299
35 Triglia, T., Tham, W. H., Hodder, A. and Cowman, A. F. (2009) Reticulocyte binding protein homologues are key adhesins during erythrocyte invasion by *Plasmodium falciparum*. Cell. Microbiol. **11**, 1671–1687
36 Trager, W. and Jensen, J. (1976) Human malaria parasites in continuous culture. Science **193**, 673–675
37 Duraisingh, M. T., Triglia, T. and Cowman, A. F. (2002) Negative selection of *Plasmodium falciparum* reveals targeted gene deletion by double crossover recombination. Int. J. Parasitol. **32**, 81–89
38 Striepen, B. and Soldati, D. (2007) Genetic manipulation of *Toxoplasma gondii*. In *Toxoplasma gondii*: The Model Apicomplexan. Perspective and Methods (Weiss, L. D. and Kim, K., eds), pp. 391–418, Elsevier, Amsterdam
39 Huynh, M. H. and Carruthers, V. B. (2009) Tagging of endogenous genes in a *Toxoplasma gondii* strain lacking Ku80. Eukaryot. Cell **8**, 530–539
40 Donald, R. G. and Roos, D. S. (1993) Stable molecular transformation of *Toxoplasma gondii*: a selectable dihydrofolate reductase-thymidylate synthase marker based on drug-resistance mutations in malaria. Proc. Natl. Acad. Sci. U.S.A. **90**, 11703–11707
41 Ehlgen, F., Pham, J. S., de Koning-Ward, T., Cowman, A. F. and Ralph, S. A. (2012) Investigation of the *Plasmodium falciparum* food vacuole through inducible expression of the chloroquine resistance transporter (PfCRT). PLoS ONE **7**, e38781
42 Tonkin, C., van Dooren, G., Spurck, T., Struck, N., Good, R., Handman, E., Cowman, A. and McFadden, G. (2004) Localization of organellar proteins in *Plasmodium falciparum* using a novel set of transfection vectors and a new immunofluorescence fixation method. Mol. Biochem. Parasitol. **137**, 13–21
43 Reference deleted
44 Bohman, K. and Isaksson, L. A. (1979) Temperature-sensitive mutants in cysteinyl-tRNA ligase of *E. coli* K-12. Mol. Gen. Genet. **176**, 53–55
45 Hou, Y. M., Westhof, E. and Giege, R. (1993) An unusual RNA tertiary interaction has a role for the specific aminoacylation of a transfer RNA. Proc. Natl. Acad. Sci. U.S.A. **90**, 6776–6780
46 Fechter, P., Rudinger, J., Giege, R. and Theobald-Dietrich, A. (1998) Ribozyme processed tRNA transcripts with unfriendly internal promoter for T7 RNA polymerase: production and activity. FEBS Lett. **436**, 99–103
47 Gardner, M., Hall, N., Fung, E., White, O., Berriman, M., Hyman, R., Carlton, J., Pain, A., Nelson, K., Bowman, S. et al. (2002) Genome sequence of the human malaria parasite *Plasmodium falciparum*. Nature **419**, 498–511
48 Eriani, G., Dirheimer, G. and Gangloff, J. (1991) Cysteinyl-tRNA synthetase: determination of the last *E. coli* aminoacyl-tRNA synthetase primary structure. Nucleic Acids Res. **19**, 265–269
49 Davidson, E., Caffarella, J., Vitseva, O., Hou, Y. M. and King, M. P. (2001) Isolation of two cDNAs encoding functional human cytoplasmic cysteinyl-tRNA synthetase. Biol. Chem. **382**, 399–406
50 Liu, C., Gamper, H., Shtivelband, S., Hauenstein, S., Perona, J. J. and Hou, Y.-M. (2007) Kinetic quality control of anticodon recognition by a eukaryotic aminoacyl-tRNA synthetase. J. Mol. Biol. **367**, 1063–1078
51 Abrahamsen, M. S., Templeton, T. J., Enomoto, S., Abrahante, J. E., Zhu, G., Lancto, C. A., Deng, M., Liu, C., Widmer, G., Tzipori, S. et al. (2004) Complete genome sequence of the apicomplexan, *Cryptosporidium parvum*. Science **304**, 441–445
52 Cavalier-Smith, T. (1999) Principles of protein and lipid targeting in secondary symbiogenesis: euglenoid, dinoflagellate, and sporozoan plastid origins and the eukaryote family tree. J. Eukaryot. Microbiol. **46**, 347–366
53 Waller, R. F., Keeling, P. J., Donald, R. G., Striepen, B., Handman, E., Lang-Unnasch, N., Cowman, A. F., Besra, G. S., Roos, D. S. and McFadden, G. I. (1998) Nuclear-encoded proteins target to the plastid in *Toxoplasma gondii* and *Plasmodium falciparum*. Proc. Natl. Acad. Sci. U.S.A. **95**, 12352–12357
54 Bartfai, R., Hoeijmakers, W. A., Salcedo-Amaya, A. M., Smits, A. H., Janssen-Megens, E., Kaan, A., Treeck, M., Gilberger, T. W., Francoijs, K. J. and Stunnenberg, H. G. (2010) H2A.Z demarcates intergenic regions of the *Plasmodium falciparum* epigenome that are dynamically marked by H3K9ac and H3K4me3. PLoS Pathog. **6**, e1001223
55 Esseiva, A. C., Naguleswaran, A., Hemphill, A. and Schneider, A. (2004) Mitochondrial tRNA Import in *Toxoplasma gondii*. J. Biol. Chem. **279**, 42363–42368
56 Nair, S. C., Brooks, C. F., Goodman, C. D., Strurm, A., McFadden, G. I., Sundriyal, S., Anglin, J. L., Song, Y., Moreno, S. N. J. and Striepen, B. (2011) Apicoplast isoprenoid precursor synthesis and the molecular basis of fosmidomycin resistance in *Toxoplasma gondii*. J. Exp. Med. **208**, 1547–1559
57 Agrawal, S., van Dooren, G. G., Beatty, W. L. and Striepen, B. (2009) Genetic evidence that an endosymbiont-derived endoplasmic reticulum-associated protein degradation (ERAD) system functions in import of apicoplast proteins. J. Biol. Chem. **284**, 33683–33691
58 Ponpuak, M., Klemba, M., Park, M., Gluzman, I. Y., Lamppa, G. K. and Goldberg, D. E. (2007) A role for falcilysin in transit peptide degradation in the *Plasmodium falciparum* apicoplast. Mol. Microbiol. **63**, 314–334
59 Kehr, S., Sturm, N., Rahlfs, S., Przyborski, J. M. and Becker, K. (2010) Compartmentation of redox metabolism in malaria parasites. PLoS Pathog. **6**, e1001242
60 Ruan, B., Nakano, H., Tanaka, M., Mills, J. A., DeVito, J. A., Min, B., Low, K. B., Battista, J. R. and Soll, D. (2004) Cysteinyl-tRNA(Cys) formation in *Methanocaldococcus jannaschii*: the mechanism is still unknown. J. Bacteriol. **186**, 8–14
61 Lee, C. P., Mandal, N., Dyson, M. R. and RajBhandary, U. L. (1993) The discriminator base influences tRNA structure at the end of the acceptor stem and possibly its interaction with proteins. Proc. Natl. Acad. Sci. U.S.A. **90**, 7149–7152
62 Hou, Y. M. and Schimmel, P. (1992) Novel transfer RNAs that are active in *Escherichia coli*. Biochemistry **31**, 4157–4160
63 Christian, T., Lipman, R. S., Evilia, C. and Hou, Y. M. (2000) Alternative design of a tRNA core for aminoacylation. J. Mol. Biol. **303**, 503–514
64 Reference deleted
65 Liu, C., Gamper, H., Liu, H., Cooperman, B. S. and Hou, Y. M. (2011) Potential for interdependent development of tRNA determinants for aminoacylation and ribosome decoding. Nat. Commun. **2**, 329
66 Hou, Y. M., Lipman, R. S. and Zarutskie, J. A. (1998) A tRNA circularization assay: evidence for the variation of the conformation of the CCA end. RNA **4**, 733–738
67 Hou, Y. M. and Schimmel, P. (1989) Evidence that a major determinant for the identity of a transfer RNA is conserved in evolution. Biochemistry **28**, 6800–6804
68 Gershon, P. D. and Howells, R. E. (1986) Mitochondrial protein synthesis in *Plasmodium falciparum*. Mol. Biochem. Parasitol. **18**, 37–43
69 Chaubey, S., Kumar, A., Singh, D. and Habib, S. (2005) The apicoplast of *Plasmodium falciparum* is translationally active. Mol. Microbiol. **56**, 81–89
70 Keller, T. L., Zocco, D., Sundrud, M. S., Hendrick, M., Edenius, M., Yum, J., Kim, Y. J., Lee, H. K., Cortese, J. F., Wirth, D. F. et al. (2012) Halofuginone and other febrifugine derivatives inhibit prolyl-tRNA synthetase. Nat. Chem. Biol. **8**, 311–317
71 Hoepfner, D., McNamara, C. W., Lim, C. S., Studer, C., Riedl, R., Aust, T., McCormack, S. L., Plouffe, D. M., Meister, S., Schuierer, S. et al. (2012) Selective and specific inhibition of the *Plasmodium falciparum* lysyl-tRNA synthetase by the fungal secondary metabolite cladosporin. Cell Host Microbe **11**, 654–663
72 Hoen, R., Novoa, E. M., Lopez, A., Camacho, N., Cubells, L., Vieira, P., Santos, M., Marin-Garcia, P., Bautista, J. M., Cortes, A. et al. (2013) Selective inhibition of an apicoplastic aminoacyl-tRNA synthetase from *Plasmodium falciparum*. ChemBioChem **14**, 499–509
73 Otoguro, K., Ui, H., Ishiyama, A., Kobayashi, M., Togashi, H., Takahashi, Y., Masuma, R., Tanaka, H., Tomoda, H., Yamada, H. and Omura, S. (2003) *In vitro* and *in vivo* antimalarial activities of a non-glycosidic 18-membered macrolide antibiotic, borrelidin, against drug-resistant strains of Plasmodia. J. Antibiot. (Tokyo) **56**, 727–729
74 Pfefferkorn, E. R. and Borotz, S. E. (1994) Comparison of mutants of *Toxoplasma gondii* selected for resistance to azithromycin, spiramycin, or clindamycin. Antimicrob. Agents Chemother. **38**, 31–37
75 Fichera, M. E., Bhopale, M. K. and Roos, D. S. (1995) *In vitro* assays elucidate peculiar kinetics of clindamycin action against *Toxoplasma gondii*. Antimicrob. Agents Chemother. **39**, 1530–1537


Received 1 November 2013/10 January 2014; accepted 16 January 2014
Published as BJ Immediate Publication 16 January 2014, doi:10.1042/BJ20131451

Biochem. J. (2014) **458**, 513–523 (Printed in Great Britain) doi:10.1042/BJ20131451

online data

## SUPPLEMENTARY ONLINE DATA

# A dual-targeted aminoacyl-tRNA synthetase in *Plasmodium falciparum* charges cytosolic and apicoplast tRNA$^{Cys}$

James S. PHAM*, Reiko SAKAGUCHI†, Lee M. YEOH*‡, Nilushi S. DE SILVA*[1], Geoffrey I. McFADDEN‡, Ya-Ming HOU† and Stuart A. RALPH*[2]

*Department of Biochemistry and Molecular Biology, Bio21 Molecular Science and Biotechnology Institute, The University of Melbourne, Melbourne, VIC 3010, Australia
†Department of Biochemistry and Molecular Biology, Thomas Jefferson University, Philadelphia, PA 19107, U.S.A.
‡School of Botany, The University of Melbourne, Melbourne, VIC 3010, Australia

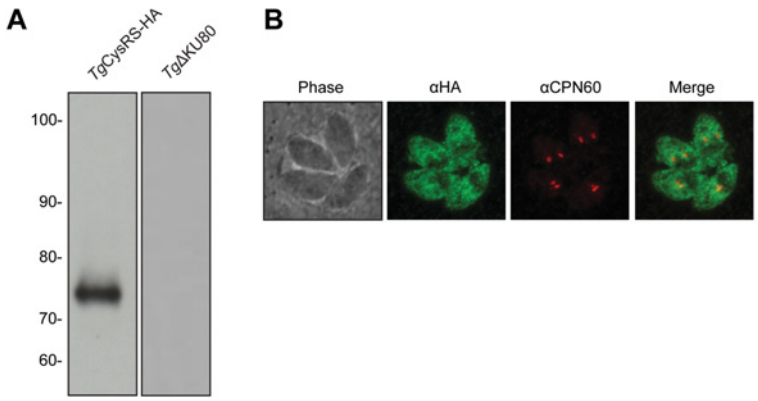


**Figure S1 Epitope tagging and localization of the *Toxoplasma gondii* CysRS**

(**A**) Western blot analysis of *Tg*CysRS–HA integrant in *T. gondii* ΔKU80 using an anti-HA antibody against the indicated parasites. A specific band is seen which is smaller than the protein predicted from the full-length gene, and thus probably corresponds to initiation from an internal methionine residue. (**B**) Immunofluorescence analysis of *Tg*CysRS–HA integrant in *T. gondii* ΔKU80. The apicoplast was stained with an anti-Cpn60 antibody. Overlap is observed between the *Tg*CysRS–HA and the Cpn60 label, but the diameter of the apicoplast is less than the spatial resolution of light microscopy, so we cannot definitively assign co-localization from these experiments.

[1] Present address: Department of Microbiology and Immunology, Columbia University Medical Center, New York, NY 10032, U.S.A.
[2] To whom correspondence should be addressed (email saralph@unimelb.edu.au).

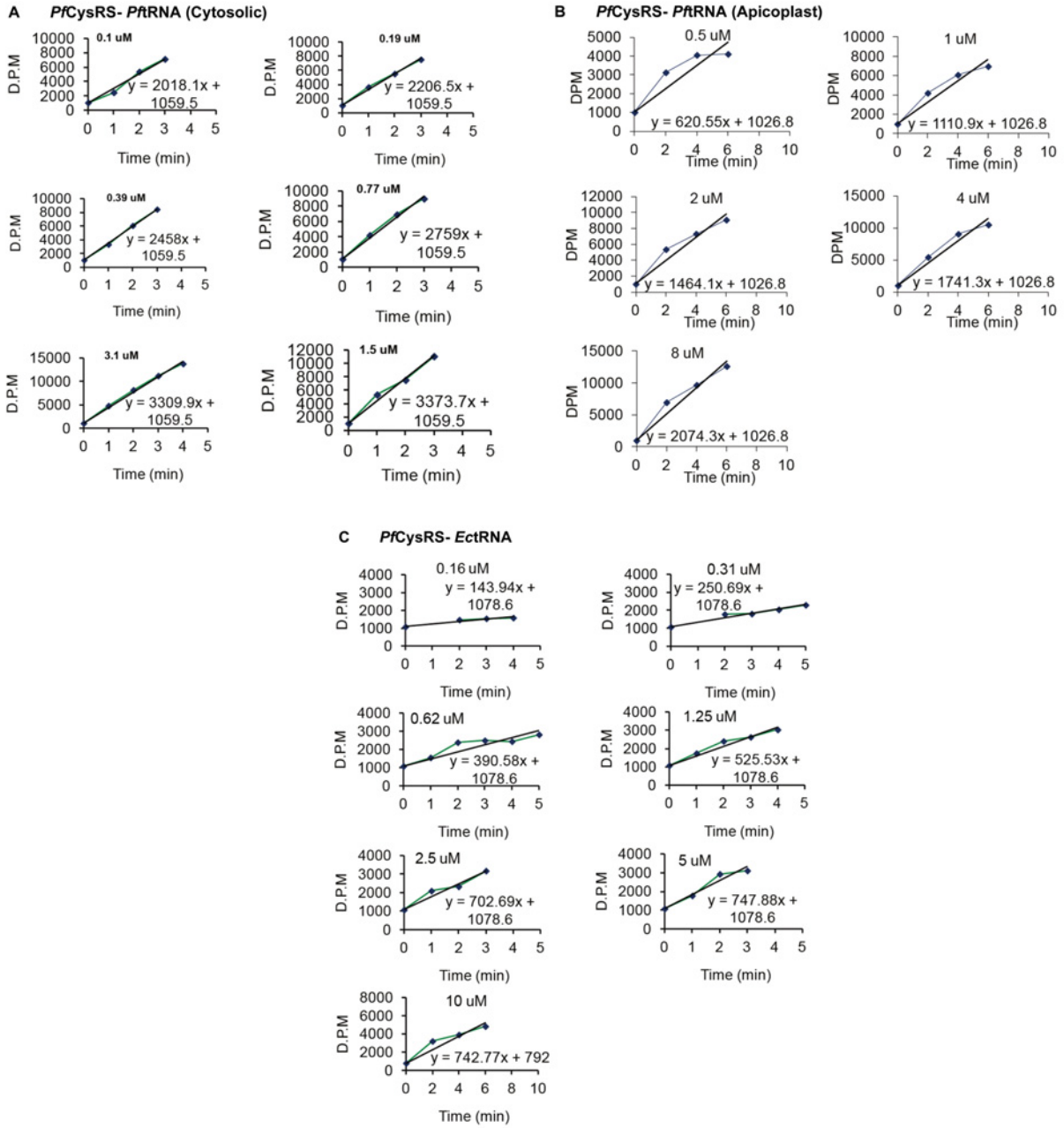


**Figure S2 Aminoacylation assays showing charging by recombinant *Pf*CysRS**

Aminoacylation, as measured by the amount of $tRNA^{Cys}$ charged with [$^{35}$S]cysteine (shown as d.p.m.) is plotted against time. Data are shown for various concentrations of substrate for each of (**A**) *P. falciparum* $tRNA^{Cys}$ (cytosolic), (**B**) *P. falciparum* $tRNA^{Cys}$ (apicoplast) and for (**C**) *E. coli* $tRNA^{Cys}$ (cytoplasm).

Received 1 November 2013/10 January 2014; accepted 16 January 2014
Published as BJ Immediate Publication 16 January 2014, doi:10.1042/BJ20131451